Picosecond Linear Dichroism and Absorption Anisotropy of Hypocrellin: Toward a Unified Picture of the Photophysics of Hypericin and Hypocrellin

K. Das, A. V. Smirnov, M. D. Snyder, and J. W. Petrich*

Department of Chemistry, Iowa State University, Ames, Iowa 50011

Received: November 18, 1997; In Final Form: May 13, 1998

The photophysics of hypocrellin is examined by means of transient absorption spectroscopy. On the shortest time scale investigated, an ~10 ps component is observed in the isotropic ("magic angle") transient absorption, $\Delta A(t)$, and in the anisotropy decay, $r(t)$, for hypocrellin in viscous solvents such as octanol and ethylene glycol. Because the excited-state intramolecular proton-transfer time of the related compound hypericin is ~10 ps, the observation of a transient of similar duration in hypocrellin is interpreted as evidence that the photophysics of hypericin and hypocrellin have common features. In particular, it is suggested that their ground- and excited-state potential energy surfaces are similar and that what distinguishes the observed kinetic behavior, which can differ significantly, is the ground-state heterogeneity, that is, the number and population of different forms of hypericin or hypocrellin, which may be tautomers, ions, or conformational isomers.

Introduction

The naturally occurring polycyclic quinones hypericin and hypocrellin (Figure 1) are of current interest because of their light-induced[1] antiviral (especially anti-HIV) and antitumor activity.[2−11] In addition, hypericin has attracted attention for its antidepressant activity.[12−15] We have discussed elsewhere several aspects of the excited-state photophysics of hypocrellin and hypericin[16−25] and have proposed means of exploiting these properties.[26,27] These molecules have been the subject of several reviews.[27−30]

It has been shown that the antiviral and antitumor activities of hypericin can be dependent on oxygen.[9,10] However, the mechanism of action of hypericin at the cellular level still remains unclear. Usually photosensitization processes involve molecules having a high triplet yield.[31] The triplet state of a photosensitizer, such as hypericin, may induce two different kinds of common and well-known photoreactions. The first and perhaps most common is the so-called type II, oxygen-dependent, mechanism. Singlet oxygen formation occurs via energy transfer from the triplet state of the photosensitizer to the ground triplet state of molecular oxygen. The second is the type I radical mechanism. This complex mechanism involves the superoxide anion[32−37] and, when hypericin is the photosensitizer, perhaps the hypericinium ion.

In addition to the well-known type I and II mechanisms, alternative origins for the photoinduced biological activity of hypericin and hypocrellin have recently been proposed.[38−42,71] Comparative studies for nine perylenequinones, including hypocrellin and hypericin, provide evidence that the quantum yield of singlet oxygen formation is not sufficient to explain the reported antiviral activities of these molecules and that other structural features of perylenequinones are involved.[43] In fact, the quantum yield of singlet oxygen from hypericin is much less than had initially been presumed. Recently, Jardon and co-workers have revised their earlier estimation of a singlet oxygen quantum yield of 0.73,[32] essentially equal to the triplet yield, to 0.35 in ethanol and less than 0.02 in water.[44] On the basis of this result, mechanisms involving oxygen clearly cannot explain all the activity of hypericin.

It has been our thesis from the very first that a significant nonradiative process in hypericin and its analogues is intramolecular proton (or atom) transfer.[16−25] The argument for such a process is the following. The hypericin analogue lacking labile protons, mesonaphthobianthrone (Figure 1d), is significantly fluorescent and has optical spectra that resemble those of hypericin only when its carbonyl groups are protonated. In hypericin, the major fluorescent state grows in on a time scale of several picoseconds, as measured by the rise time of stimulated emission. Therefore, the combined observations of the requirement of protonated carbonyls for strong hypericin-like fluorescence and the rise time of fluorescence in hypericin were taken as evidence for intramolecular excited-state proton transfer in hypericin.

Of special relevance to the role of labile protons for the light-induced biological activity of hypericin is the observation that hypericin acidifies its surroundings upon light absorption.[39−42,71] The role of photogenerated protons takes on significance in the context of the growing body of literature implicating pH decreases with pharmacologically important functions, such as virucidal activity (optimum pH values are important in the life cycles of many enveloped viruses),[45] antitumor activity,[46,47] apoptosis (a form of cell death associated with DNA fragmentation and chromatin condensation),[48−50] and the subcellular distribution of hexokinase.[51] In this light, current work on subcellular localization of hypericin[52] and the interaction of hypericin with DNA[53−55] and proteins[56−58] is of considerable interest.

The structural similarities of hypocrellin and hypericin, especially the hydroxyl groups *peri* to the keto groups, may initially give the impression that these two molecules exhibit very similar excited-state photophysics. This is not the case, and the photophysics of these molecules is compared and contrasted in section A of the Discussion. Because of the different behavior manifested by the proton-transfer reactions

* To whom correspondence should be addressed.

S1089-5647(98)00249-1 CCC: $15.00
Published on Web 07/11/1998

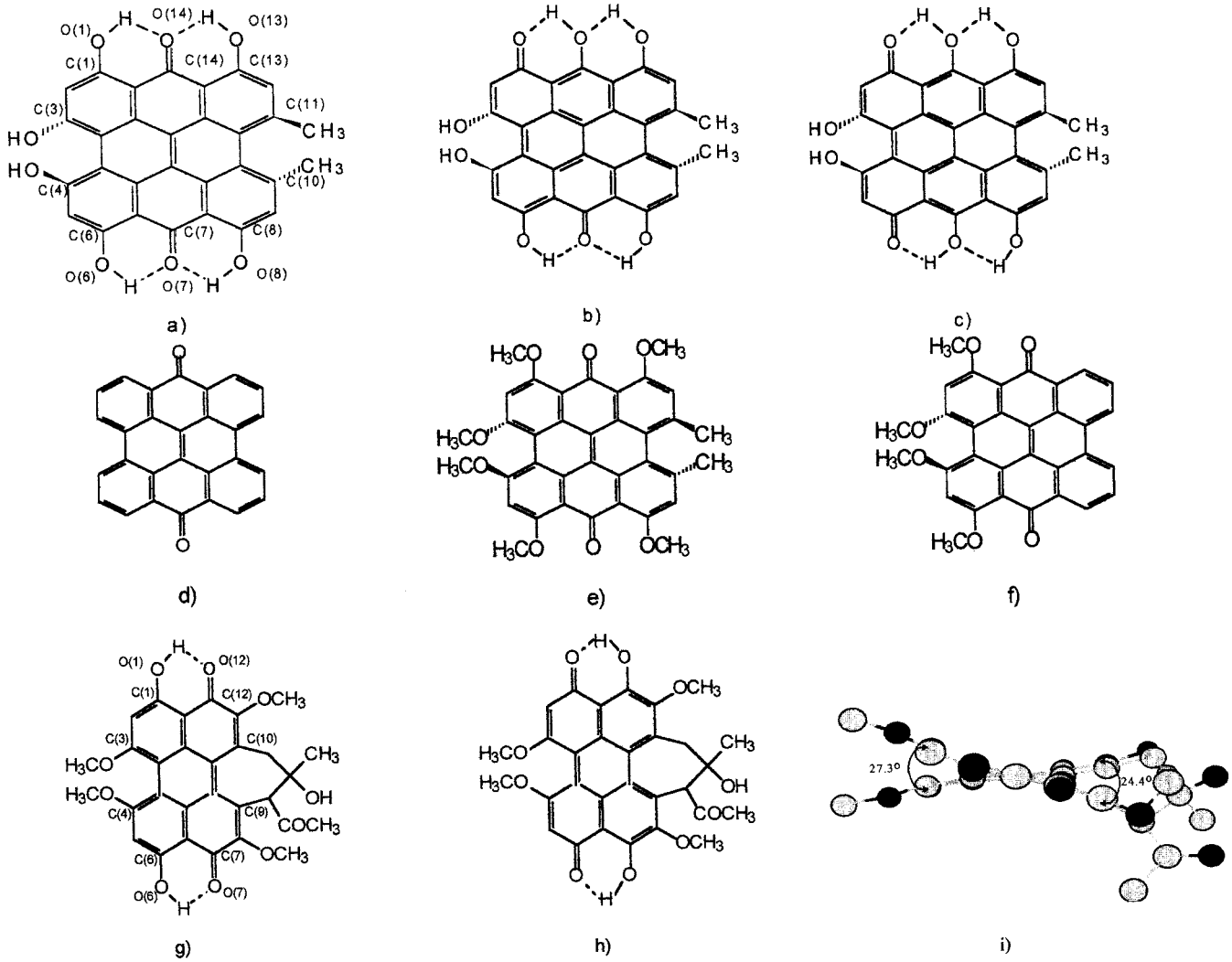

Figure 1. Two-dimensional structures of (a) "normal" form of hypericin, (b) one of the two possible hypericin mono tautomers, (c) one of the three possible hypericin double tautomers, (d) mesonaphthobianthrone (phenanthro[1,10,9,8,*o,p,q,r,a*]perylene-7−14-dione), (e) *O*-hexamethoxy hypericin, (f) *O*-tetramethoxy hypericin, (g) two-dimensional structures of the "normal" form of hypocrellin A, and (h) the double tautomer of hypocrellin. The distortion of the hypocrellin skeleton due to the interactions of the side chain groups is indicated in (i). For hypocrellin, twist angles of 27.3° and 24.4° are measured with respect to C(3) and C(4) and C(9) and C(10), respectively.[64,65] Comparable twist angles are observed in hypericin.[63,70]

in hypericin and hypocrellin, these two molecules provide unique systems with which to clarify and to understand aspects of proton-transfer reactions, which have been a subject of much experimental and theoretical study. An important goal, consequently, is to construct a *unified* and self-consistent model of the ground- and excited-state potential surfaces of hypericin and hypocrellin, with the aim of describing the proton or atom transfer in this class of polycyclic quinones. Such a model should necessarily include information on the number of ground-state species of hypocrellin and hypericin and which of them interconvert upon optical excitation. To address these topics, time-resolved experiments with polarized pump and probe pulses have been performed, from which anisotropy functions are constructed. If the excited-state tautomerization process is accompanied by a conformational or other change that induces a change in the transition dipole moment, this change should be detected in the polarized absorption data. Such effects are indeed observed in hypocrellin, as noted below. Measuring the time-dependent anisotropy thus permits a mapping out of the excited-state potential energy surface and a characterization of the species involved in the excited-state proton transfer.

Experimental Section

Hypocrellin A was obtained from Molecular Probes. Time-resolved linear dichroism experiments are performed with amplified dye laser pulses of ∼1−3 ps duration at 30 Hz.[21] The time-resolved anisotropy of the hypocrellin transients was constructed for two solvents, ethanol and octanol, and was studied on time scales ranging from 40 ps to 2 ns (Tables 1 and 2). In these experiments the polarization of the probe was always kept constant, while the polarization of the pump (588 nm) was rotated. A photodiode was employed to integrate the pump energy in order to provide a shot-to-shot normalization of the intensities of the polarized kinetic traces.

The anisotropy was obtained as follows. All the parallel traces were globally fitted, and the time constants and respective amplitudes were extracted. For the perpendicular traces, the transient at 595 nm is different from the other traces (570, 560, and 550 nm). Thus, the 595 nm trace was fit individually and the other three traces were fit globally, from which time constants and amplitudes were extracted. From those respective amplitudes and time constants deconvoluted decay curves for parallel and perpendicular polarization were constructed and finally the "magic angle" decay curves were constructed as

TABLE 1: Magic Angle Decay Parameters for Hypocrellin[a]

solvent	time scale(ps)[c]	λ_{probe} (nm)	a_1	τ_1 (ps)	a_2	τ_2 (ps)[b]
ethanol	200	595	-0.014 ± 0.001	80 ± 5	-0.001 ± 0.0005	∞
		570	-0.06 ± 0.02	80 ± 5	0.01 ± 0.005	∞
		560	-0.08 ± 0.02	80 ± 5	0.02 ± 0.01	∞
		550	-0.08 ± 0.01	80 ± 5	0.02 ± 0.004	∞
octanol	40	570	-0.03 ± 0.01	8 ± 1	0.007 ± 0.001	∞
		560	-0.05 ± 0.02	8 ± 1	0.005 ± 0.0003	∞
		550	-0.03 ± 0.01	8 ± 1	0.001 ± 0.0003	∞
	500	595	-0.05 ± 0.02	230 ± 18	-0.001 ± 0.0004	∞
		570	-0.087 ± 0.03	230 ± 18	0.02 ± 0.003	∞
		560	-0.097 ± 0.02	230 ± 18	0.01 ± 0.001	∞
		550	-0.05 ± 0.01	230 ± 18	0.01 ± 0.001	∞

[a] $\lambda_{pump} = 588$ nm. [b] Time constant for this second component is much greater than the time scale of the experiment, $\tau_2 = \infty$. The errors cited are the standard deviations of the average of several measurements, when more than one measurement was performed. [c] On some time scales only two probe wavelengths are employed for the global fit.

TABLE 2: Anisotropy Decay Parameters for Hypocrellin[a]

solvent	time scale[c] (ps)	λ_{probe} (nm)[d]	a_1	τ_1 (ps)	a_2	τ_2 (ps)[b]
ethanol	100	570	-0.34	129	-0.22	∞
		560	-0.25	129	-0.1	∞
	200	570	-0.18 ± 0.05	118 ± 6	-0.36 ± 0.04	∞
		560	-0.20 ± 0.02	118 ± 6	0.001 ± 0.001	∞
		550	-0.21 ± 0.02	118 ± 6	0.003 ± 0.001	∞
	2000	560	-0.12	176	-0.11	∞
		550	-0.09	176	-0.11	∞
octanol	40	570	-0.20 ± 0.1	6.3 ± 0.3	-0.18 ± 0.06	∞
		560	-0.35 ± 0.01	6.3 ± 0.3	-0.13 ± 0.03	∞
		550	-0.24 ± 0.06	6.3 ± 0.3	-0.22 ± 0.06	∞
	500	570	-0.22	728	-0.08	∞
		560	-0.27	728	-0.04	∞
	2000	570	-0.20	774	-0.09	∞
		560	-0.10	774	-0.17	∞
		550	-0.08	774	-0.22	∞

[a] $\lambda_{pump} = 588$ nm. [b] Time constant for this second component is much greater than the time scale of the experiment, $\tau_2 = \infty$. The errors cited are the standard deviations of the average of several measurements, when more than one measurement was performed. On some time scales, only one measurement was performed. [c] On some time scales only two probe wavelengths are employed for the global fit. [d] Data for $\lambda_{probe} = 595$ nm could not be fit owing to the discontinuity incurred (see Experimental Section).

follows:

$$\Delta A(t) = \Delta A_{||}(t) + 2\Delta A_{\perp}(t)$$

The magic angle or isotropic transient absorption trace was also measured directly. This direct measurement is what is presented in Figures 3−7. The anisotropy was found as usual:

$$r(t) = \frac{\Delta A_{||}(t) - \Delta A_{\perp}(t)}{\Delta A_{||}(t) + 2\Delta A_{\perp}(t)}$$

Because the anisotropy is discontinuous at 595 nm, only the other three probe wavelengths at 570, 560, and 550 nm could be employed in a global fitting procedure to extract the amplitudes and the time constants. $\Delta A(t)$ and $r(t)$ are fit to sums of two exponentials. Some data sets are presented for hypocrellin in the respective panels of Figures 3−7. In some cases (Table 2) the absolute magnitude of the limiting anisotropy is greater than the theoretical limit of 0.40. There is nothing contradictory in such a result since this limit corresponds to a single transition in the absence of coherence effects.[59,60] A limiting anisotropy whose absolute magnitude is in excess of 0.40 thus indicates that several different transitions are being probed simultaneously. Similar results have been obtained elsewhere.[61,62]

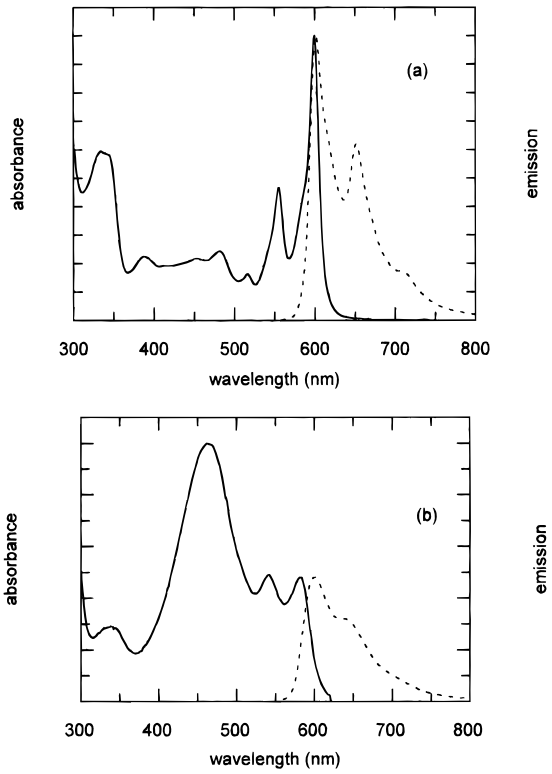

Figure 2. Normalized fluorescence spectra (dashed line) and absorption spectra (solid line) of hypericin (a) and hypocrellin (b) in DMSO. The spectra of hypocrellin and hypericin are relatively insensitive to solvent. The steady-state emission spectra bear a "mirror symmetry" relationship to the visible portion of the absorption spectrum. We attribute this symmetry to the presence of ground-state tautomers,[17] ions, or conformational isomers. Transient absorption measurements using two different excitation wavelengths are consistent with such heterogeneity.[19,20] Also consistent with this assignment is the observation that fluorescence upconversion measurements yield different kinetics at different emission wavelengths.[24]

Results

Hypocrellin transients were typically investigated at four probe wavelengths: 595, 570, 560, and 550 nm. Time constants are extracted from these four wavelengths using a global fitting routine.[21] The main features of this study are the following. At 595 nm, there is *stimulated emission* for parallel pump and probe, whereas *induced absorbance* (whose signal is much weaker) is observed for perpendicular pump and probe. As a result the anisotropy is *discontinuous* (Figure 3). At the other three probe wavelengths (570, 560, 550 nm) induced absorbance is present for both parallel and perpendicular probe polarizations. However, the intensity for the perpendicular orientation is always *greater* than that of parallel, resulting in a negative anisotropy at these wavelengths. In viscous solvents (e.g., octanol) the parallel transients at 570, 560, and 550 also have a fast rise time (∼7 ps) which is absent in the perpendicular traces.

Discussion

A. Intramolecular Proton Transfer. We have provided the first detailed investigations that use both ≤1 ps time resolution and white-light continuum to examine and to unravel the excited-state *primary photoprocesses* of hypericin and hypocrellin and have argued that the excited-state transients we observe, coupled with data from model compounds, can be interpreted in terms of excited-state tautomerization.[16−25] The

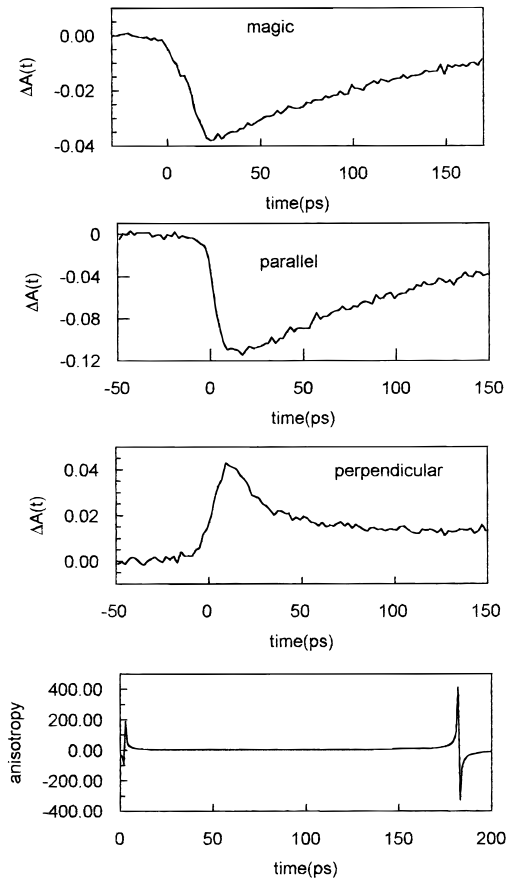

Figure 3. Transient absorption of hypocrellin in ethanol: $\lambda_{pump} = 588$ nm, $\lambda_{probe} = 595$ nm. Note that the sign of the perpendicular trace is opposite that of the parallel and magic angle traces.

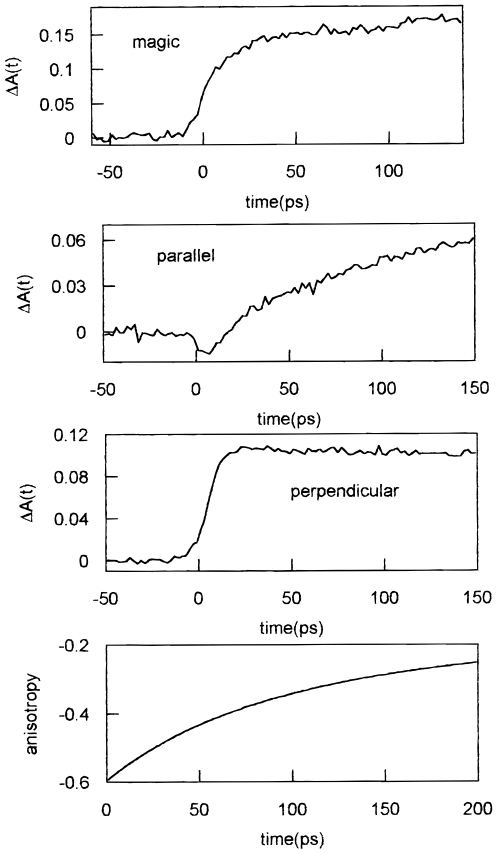

Figure 4. Transient absorption of hypocrellin in ethanol: $\lambda_{pump} = 588$ nm, $\lambda_{probe} = 570$ nm.

structural similarities of hypocrellin and hypericin, especially the hydroxyl groups *peri* to the keto groups, may initially give the impression that these two molecules exhibit very similar excited-state photophysics. We have made the following observations and conclusions.

1. The deshydroxy analogue of hypericin, mesonaphthobianthrone (phenanthro[1,10,9,8,*o,p,q,r,a*]perylene-7,14-dione (Figure 1d), is nonfluorescent except in strong acids [e.g., sulfuric acid or triflic acid (CF_3SO_3H)], where it produces a fluorescence spectrum that has nearly the same shape as that of hypericin in DMSO (Figure 2). *These results demonstrate the importance of a protonated carbonyl group for producing hypericin-like fluorescence.*[17,24]

2. The hypericin emission spectrum at 600 nm grows in on a 6−12 ps time scale in all solvents except in sulfuric acid where it is instantaneous. On the basis of the results for mesonaphthobianthrone (see above), *the rise time for the appearance of the hypericin emission is taken as evidence for an excited-state proton (atom) transfer.*[17] Confirming this interpretation are the fluorescence upconversion measurements[24] of hypericin and methylated hypericin analogues, which are incapable of executing intramolecular excited-state proton-transfer reactions.

3. The transient absorbance[19,20] and upconversion[24] kinetics of hypericin differ with excitation wavelength and probe wavelength, respectively. These results are strongly suggestive of ground-state heterogeneity. Also, the fluorescence properties of hypocrellin in sulfuric acid and the X-ray structure of hypocrellin suggest that it exists in the tautomerized form in the ground state (Figure 1g).[21−23,65]

4. The proton-transfer rates of hypocrellin and hypericin differ almost by an order of magnitude. The X-ray and fluorescence data (above) consequently lead us to propose that hypocrellin exists at least partially in a tautomeric form that is similar to that which hypericin would assume in the ground state (Figure 8), if it were thermodynamically feasible. Given this assumption, the 50−230 ps transients in hypocrellin are interpreted in terms of "back transfer" reactions[64] with respect to the corresponding hypericin reaction.

5. The proton transfer reaction in hypericin is not dependent on viscosity and depends only very weakly on solvent.[18] This suggests that intramolecular vibrations control the proton transfer reaction in hypericin. However for hypocrellin the reaction is very strongly dependent on viscosity and polarity.[21,22]

6. No deuterium isotope effect is observed for hypericin;[17] but a deuterium isotope effect of 1.4 is observed for hypocrellin.[23] *This isotope effect unambiguously identifies the excited-state process as a proton-transfer event.*

7. For hypocrellin in viscous solvents such as octanol and ethylene glycol, a transient of ∼10 ps duration is also detected.[21] *This is a crucial and unifying result for understanding the photophysics of these systems.*

8. The fluorescence lifetimes of hypericin and hypocrellin, measured with ∼50 ps time resolution, are independent of excitation wavelength: identical results are obtained exciting at 300 or 570 nm.[25] Assuming that the ground states of these species are heterogeneous, as noted above, this result suggests that the fluorescent species (detected via methods with time resolution no better than 100 ps) for both hypocrellin and hypericin is an intermediate between (two) tautomeric or isomeric species.

9. The absorption transients of hypocrellin exhibit a strong polarization dependence (Figures 3 and 6) at a probe wavelength of 595 nm. While the traces obtained using the pump and probe

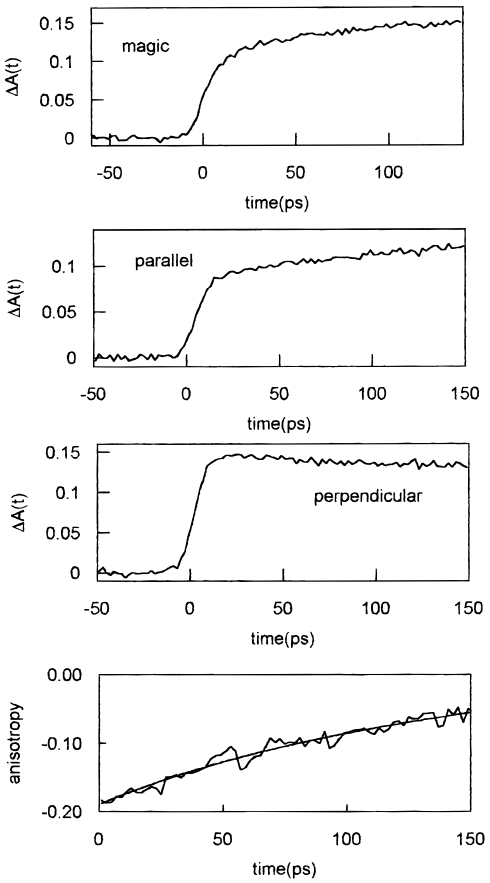

Figure 5. Transient absorption of hypocrellin in ethanol: $\lambda_{pump} = 588$ nm, $\lambda_{probe} = 550$ nm. The bottom panel compares the anisotropy calculated from the *fits* of the parallel and perpendicular traces (smooth line) with the anisotropy obtained directly from the experimental parallel and perpendicular traces (noisy line).

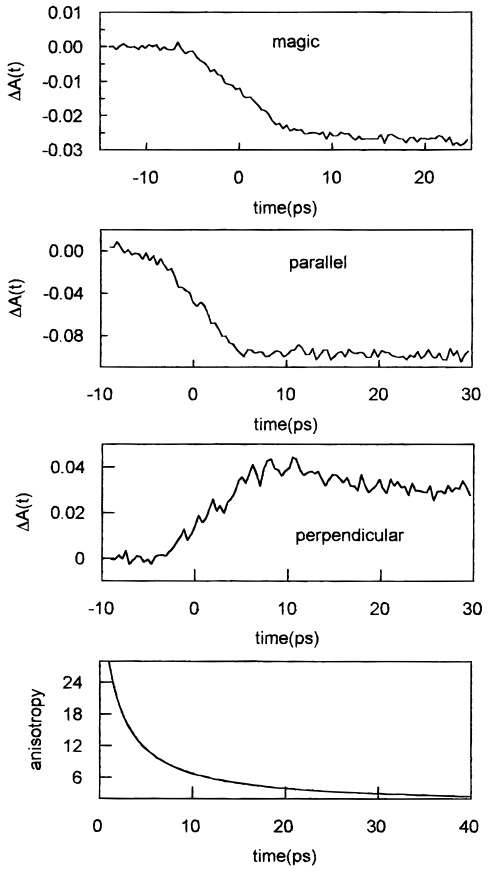

Figure 6. Transient absorption of hypocrellin in octanol: $\lambda_{pump} = 588$ nm, $\lambda_{probe} = 595$ nm. Note that the sign of the perpendicular trace is opposite that of the parallel and magic angle traces

polarized parallel to each other or at 54.7° (the "magic angle"), $\Delta A_{||}(t)$ and $\Delta A(t)$, are essentially superimposable, the trace obtained using perpendicularly polarized pump and probe pulses, $\Delta A_{\perp}(t)$ is opposite to that of the parallel and magic angle traces at 595 nm. This result indicates the simultaneous probing of two species whose transition dipole moments are at large angles to each other.

On the basis of these results and conclusions, we are constructing a unified picture of the excited-state proton-transfer phenomena in these molecules.

B. Toward a Unified Picture of the Hypericin and Hypocrellin Photophysics. Structurally, hypericin and hypocrellin are very similar. They both possess extended aromatic skeletons whose most important functional groups are the hydroxy and keto groups peri to each other. In this regard, the most significant structural difference between them is that hypocrellin possesses two fewer *peri* hydroxyl groups. (Another significant difference is that hypocrellin has a seven-membered ring in the "bay area".) The current picture that we have formed of the excited-state dynamics of hypericin and hypocrellin is that the different photophysical behavior that we have enumerated above of these two structurally very similar molecules arises because we are probing different regions of *very similar potential energy surfaces.* We suggest that at least one of the ground-state species excited in the hypocrellin experiments is very similar to the ground-state tautomer of hypericin (Figure 1b), which we propose is thermodynamically inaccessible. These ideas are summarized schematically in Figure 8. A crucial result in forming this hypothesis is the observation that in viscous solvents such as octanol or ethylene glycol we resolve a time constant in the hypocrellin photophysics that is comparable to that observed in hypericin. This ~10-ps component in hypocrellin unifies our picture of the photophysics of hypericin and hypocrellin if we can interpret it as an excited-state proton-transfer arising from another tautomeric species and if we can relate it to the corresponding process in hypericin.

The absence of a deuterium isotope effect on the excited-state proton transfer in hypericin and the presence of a deuterium isotope effect on the excited-state proton transfer in hypocrellin both can be qualitatively understood in terms of a process that is adiabatic in the proton coordinate, in the sense of the theory developed by Borgis, Hynes, and co-workers.[66−69] We have considered the excited-state potential energy surfaces of hypericin and hypocrellin in terms of this theory.[23,25]

The oxygen−oxygen distance between which the proton or hydrogen atom is transferred strongly modulates the magnitude of the matrix element that couples the reactant and product states and thus determines the size of the barrier separating them. When the O−O distance is < 2.6 Å, the *adiabatic limit* is obtained.[68,69] Here, because the vibrational energy levels of the proton stretch mode lie *above* a small barrier in the proton coordinate separating the reactant and product species, an isotope effect will not be observed as a result of proton transfer. We have argued that hypericin falls into the adiabatic limit[17,23] because its relevant oxygen−oxygen distance is ~2.5 Å.[70] In hypocrellin, this distance is comparable.[65]

Staib et al.,[69] however, suggest the intriguing possibility that deuterium substitution may lower the ground vibrational energy below the top of the barrier in the proton coordinate. Such a lowering of the ground-state energy level would induce an

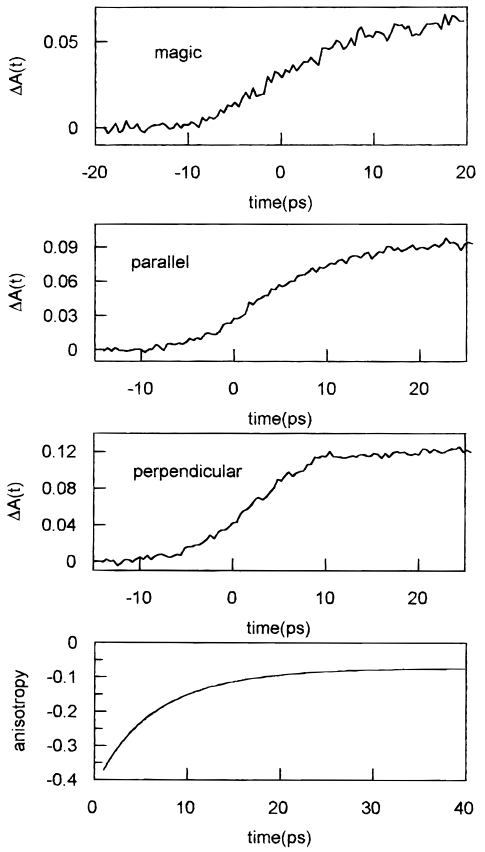

Figure 7. Transient absorption of hypocrellin in octanol: $\lambda_{pump} = 588$ nm, $\lambda_{probe} = 560$ nm.

isotope effect because now the proton could tunnel through the barrier or effect an activated crossing of it. We propose that the isotope effect observed in hypocrellin has its origins in such an explanation. That the isotope effect is relatively small suggests that the vibrational ground state is not significantly lowered below the barrier and that the proton transfer is an activated process. Temperature studies will be useful to confirm this hypothesis.

C. Simulating the Excited-State Kinetics. Our picture of the excited-state kinetics of hypocrellin, and their relation to hypericin, has evolved significantly since our early work on hypocrellin.[21] Here we present the simulations for the excited-state dynamics of hypocrellin A based upon the pump−probe transient absorbance data presented above. The unified model of the excited-state photophysics for hypericin and hypocrellin is based upon the experimental observations cited above in section A.

On the basis of the above results and conclusions, the simplest approach would be to assume that in the ground state there are two tautomers (N and T) in equilibrium. We also assume that the triplets and the excited singlets of the above-mentioned tautomers were the only species responsible for the excited-state photophysics:

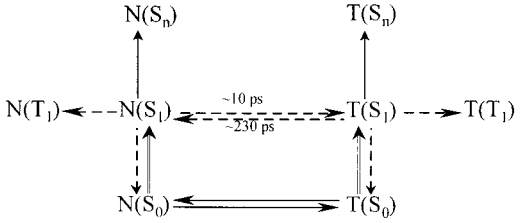

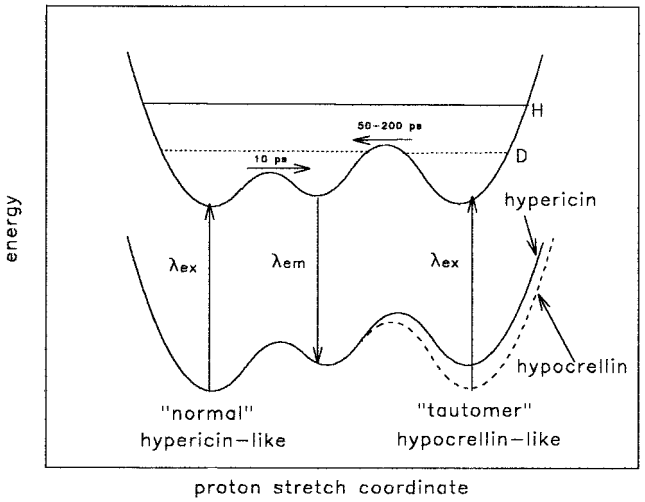

Figure 8. Unified picture depicting the ground- and excited-state potential energy surfaces for hypericin-like and hypocrellin-like molecules as a function of the proton stretch coordinate. The right-hand side of the ground-state potential energy surface depicts our proposal that the hypericin bitautomer (Figure 1c) is not populated in the ground state, whereas the hypocrellin tautomer (Figure 1h) is populated. On the excited-state surface, the zero-point vibrational levels for an OH···O or an OD···O system are depicted.[69] The height of the zero-point level with respect to the barrier in the proton stretch coordinate determines whether an isotope effect will be observed. The third potential well, the middle of the figure, represents either another possible tautomeric form or some other intermediate between, for example, the normal and the fully or bitautomer species of hypericin. The arrows in the diagram are meant to remind the reader of the time constants for the proton-transfer processes in hypericin and hypocrellin. One should not identify the proton coordinate for the reaction coordinate in this system

At best this model is capable of providing one rapidly rising or decaying component and one slowly decaying component (to the triplet or the ground state). Solvent relaxation processes can be viewed as negligible here since no Stokes shift was observed for the hypocrellin analogue, hypericin, in fluorescence upconversion measurements with 100 fs time resolution.[24] The above model is not, therefore, consistent with our observation of at least three different transient components for hypocrellin on time scales from 40 to 2000 ps.

Consequently, it is necessary to introduce at least one more species into the kinetic scheme. In this new model the main feature is the intermediate tautomer (or conformational isomer) $I(S_1)$ that is produced from both $N(S_1)$ and $T(S_1)$.

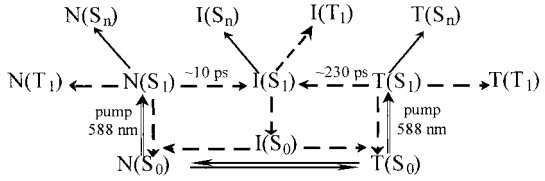

Other alternatives for the excited-state kinetic scheme presented above include:

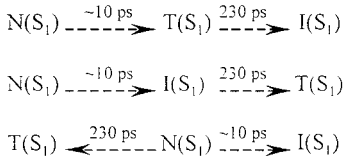

These alternative schemes are readily eliminated *if we assume that N(S_1) and T(S_1) have similar absorption and emission spectra, and if we interpret the experimental kinetic traces as arising from an intermediate I(S_1).* If this is the case, no contribution to the 10 ps and/or 230 ps components should be observed when N(S_1) and T(S_1) interconvert into each other directly, or indirectly through I(S_1). For example, in the first and third alternatives, if N(S_1) decays into T(S_1), equivalence of the excited-state spectra will render the transition undetectable. The second alternative is merely equivalent to an excited-state equilibrium of N(S_1) with I(S_1).

To evaluate the model, we performed computer simulations in an attempt to reproduce the main features of the data obtained for hypocrellin in ethylene glycol. First we solved the system of the first-order ordinary differential equations as dictated by our kinetic scheme. Then we used the resulting time-dependent populations of the species involved to construct parallel and perpendicular transient absorbance traces. This required the use of different values of the extinction coefficients (for absorbance and stimulated emission) for different probe wavelengths. To allow for the possibility of *negative* initial absorbance anisotropy for hypocrellin, one has to assign in the first approximation orthogonality of transition dipole moments from the ground to the first excited and from the first excited to the second excited states. This can be also viewed as a consequence of the nearly C_{2v} symmetry of hypocrellin. In our model, each of the excited-state singlets is characterized by two orthogonal extinction coefficients, $\epsilon_{||}$ and $\epsilon_{\perp}$. More specifically, when probing at 595 nm, the parallel component ($\epsilon_{||}$) is made negative to account for the dominating contribution of stimulated emission. On the other hand, the perpendicular component ($\epsilon_{\perp}$) is made positive to account for the excited-state absorption that was present in all the data collected for perpendicular probe polarizations. It is assumed that all triplet states have very similar absorption spectra and that they do not contribute to the stimulated emission.

Depolarization owing to rotational diffusion of hypocrellin was taken into account ($\tau_R \sim 100-800$ ps, depending on the solvent). Other mechanisms of depolarization were also taken into account: namely, conversion of one tautomer to another or intersystem crossing to the triplet state. In terms of our model this leads to the conclusion that the transition dipole for I(S_0) $\leftrightarrow$ I(S_1) is in fact at some angle relative to that for N(S_0) $\leftrightarrow$ N(S_1) and T(S_0) $\leftrightarrow$ T(S_1).

To model the rotational diffusion, we assumed hypocrellin to be a spherical rotor and used the general formalism developed by Chuang and Eisenthal[72] for an asymmetric rotor for fluorescence depolarization, which we extended in our case to the pump/probe experiments discussed here. For each species the corresponding contribution to the signal for the appropriate polarization is given by

$$\Delta A_{i,||}(t) = Pi_{,||}(t)\left(\frac{1}{9} + \frac{2}{45}(3\cos^2\theta_{i,||} - 1)e^{-t/\tau_r}\right) + P_{i,\perp}(t)\left(\frac{1}{9} + \frac{2}{45}(3\cos^2\theta_{i,\perp} - 1)e^{-t/\tau_r}\right)$$

$$\Delta A_{i,\perp}(t) = P_{i,||}(t)\left(\frac{1}{9} - \frac{1}{45}(3\cos^2\theta_{i,||} - 1)e^{-t/\tau_r}\right) + P_{i,\perp}(t)\left(\frac{1}{9} - \frac{1}{45}(3\cos^2\theta_{i,\perp} - 1)e^{-t/\tau_r}\right)$$

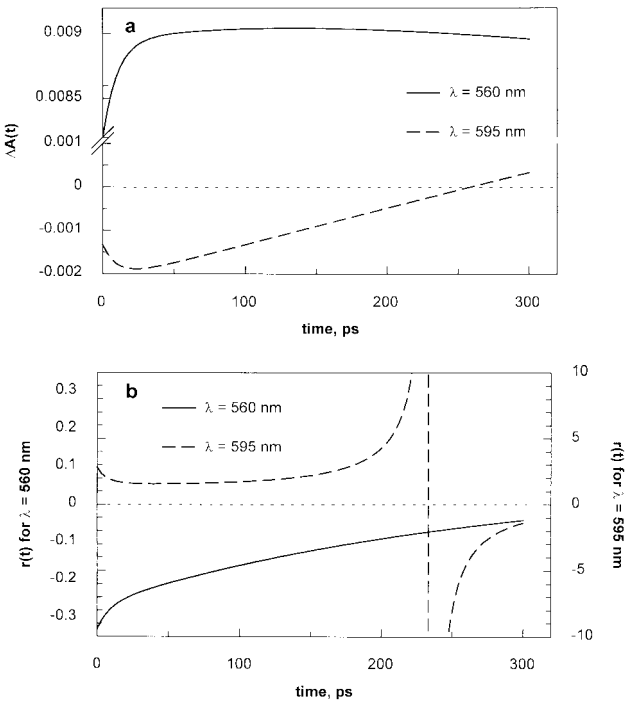

Figure 9. Results of simulations based on the kinetic scheme proposed in the text. Isotropic ("magic angle") transient absorption (a), $\Delta A(t)$, of hypocrellin in octanol at $\lambda_{probe} = 560$ and 595 nm. Anisotropy decay (b), $r(t)$, of hypocrellin in octanol at $\lambda_{probe} = 560$ and 595 nm. Note the discontinuity for the 595 nm trace at around 230 ps. These simulated traces when compared with their experimental counterparts (data not shown for octanol at longer time scales) show that the salient features of the kinetics are qualitatively reproduced in all cases. It may be noted that the zero-crossing time for the magic angle simulation trace does not match exactly the discontinuity in the anisotropy at 595 nm. This is not a discrepancy in the simulation but a result of the approach we used to find suitable parameters for the proposed model. At first, isotropic quantities were varied to reproduce the general shape and magnitude of the magic angle trace, and then these quantities were fixed to find anisotropy-related parameters that follow the general, qualitative trends of the anisotropy constructed from the experimental data. In this final step, our main focus was the early-time behavior of the anisotropy and the presence (but not the quantitative position in time) of the discontinuity. From our point of view this approach is justified within the limits of the experimental uncertainty. We note that the aim of these simulations was to reproduce qualitative features of the data and not to fit them.

$$P_{i,||}(t) = \epsilon_{i,||}P_i(t) \qquad P_{i,\perp}(t) = \epsilon_{i,\perp}P_i(t)$$

where $P_i(t)$ is the probability for the species with transition dipoles oriented at angles $\theta_{i,||}$ and $\theta_{i,\perp}$ relative to the ground-state absorption to survive by the time t.

In a program written for Maple V, we simulated both perpendicular and parallel transient absorption traces, from which the anisotropy decay was constructed. No convolution procedure was necessary for our purposes, given the time scale of the simulations. Semiquantitative values for the $\epsilon_{||}$ and $\epsilon_{\perp}$ are obtained by trial and error method. Time-dependent plots of intermediate populations are used as guidelines for this multiparametric search. Separate simulations with globally fixed temporal and orientational parameters for the transition dipoles were performed for each probing wavelength until a reasonable agreement with experimental data was achieved. Figure 9 describes the simulation results; the parameters are listed in Table 3. It should be noted that although we were able to reproduce qualitatively the anisotropy and stimulated emission features, the absorbance features do not agree quantitatively with the experimental observations.

TABLE 3: Parameters and Results for the Simulations of Hypocrellin Photophysics

parameter	
type	value
$N(S_1) \rightarrow I(S_1)$[a]	10 ps
$T(S_1) \rightarrow I(S_1)$[a]	230 ps
rotational diffusion time[a]	800 ps
$S_1 \rightarrow S_0$ inverse radiative rate [b]	7000 ps
inverse intersystem crossing rate[b]	1000 ps
transition dipole shift for $I(S_0) \leftrightarrow I(S_1)$	$\sim \pi/4$[c]

results			
	probe wavelength		
extinction coefficient [d]	560 nm	570 nm	595 nm
$\epsilon_{N(S_1),\parallel}$	0.82	0.30	−0.15
$\epsilon_{N(S_1),\perp}$	0.95	1.90	0.92
$\epsilon_{T(S_1),\parallel}$	0.82	0.30	−0.15
$\epsilon_{T(S1),\perp}$	0.95	1.90	0.92
$\epsilon_{I(S_1)}$	0.95	0.70	−3.23
$\epsilon_{I(S_1)}$	0.95	1.80	3.68
$\epsilon_{N(T_1)}$, $\epsilon_{T(T_1)}$, $\epsilon_{I(T_1)}$	1.82	2.00	2.81

[a] Experimental observations from our laboratory. [b] Inverse of the radiative rate k_R of $N(S_1)$, $T(S_1)$, and $I(S_1)$ to the ground state. We assume k_R to be the same for all three of these species. Based on the reported[81] triplet yield of hypocrellin in benzene. [c] Shift in angle relative to the ground-state absorption dipoles of N and T that was necessary to account for lower than theoretical initial fluorescence anisotropy value. In terms of our model this leads to the conclusion that the transition dipole for $I(S_0) \leftrightarrow I(S_1)$ is in fact at some angle relative to that for $N(S_0) \leftrightarrow N(S_1)$ and $T(S_0) \leftrightarrow T(S_1)$. [d] Extinction coefficients relative to those of ground-state species, $\epsilon_{N(S_0)}$, $\epsilon_{T(S_0)}$, which are taken to be unity. All of these, except for $\epsilon_{N(T_1)}$, $\epsilon_{T(T_1)}$, and $\epsilon_{I(T_1)}$, are determined to within ± 0.05.

To summarize, the model proposed to rationalize hypocrellin transient absorbance traces proves to be self-consistent by providing reasonable parameters for the $\epsilon_{||}$ and $\epsilon_{\perp}$. Although the real picture might be much more complicated from our point of view, we found the simplest possible semiquantitative description of this remarkable photophysical system.

We stress that we have made no effort to *fit* the experimental kinetics, owing to the huge number of variable parameters, which we have noted above. We also note that the scheme provided is neither complete nor unique. It is our goal merely to reproduce qualitatively the salient features, and indeed, the scheme presented is *consistent* with our emerging picture of the hypericin and hypocrellin photophysics.

Concluding Remarks

Over the past few years our efforts have been directed toward demonstrating that a fundamental *primary photoprocess* in hypericin and its analogues that possess hydroxyl groups *peri* to keto groups is excited-state proton (or atom) transfer. This work addresses the excited-state proton transfer of hypericin and hypocrellin and attempts to incorporate their different behavior into a coherent picture. The link between the photophysics of hypericin and hypocrellin is established by the observation that under certain conditions a hypericin-like transient is observed in hypocrellin. We have proposed kinetic schemes and ground- and excited-state potential surfaces for these systems that are consistent with the experimental data.

We note that the excited-state proton-transfer reaction observed in our experiments (ranging from 10 to 200 ps) is not detectable in steady-state fluorescence experiments or even in most time-correlated single-photon-counting experiments. Consequently, it must be borne in mind that such experiments (e.g., fluorescence titrations[63,73−75]) can yield information only on the species that are formed as a result of these 10−200 ps proton-transfer processes, that is, the long-lived nanosecond-duration fluorescent species that are detected in the steady-state measurements. While steady-state fluorescence titrations cannot report on the picosecond proton-transfer events, they have been useful in demonstrating the acidity of the hydroxyls in the "bay region" of hypericin.[63,73,74]

Acknowledgment. Mr. Tak Wee Kee provided technical assistance. We thank Dr. S. Savikhin for helpful discussions. This work was supported by NSF Grant CHE-9613962 to J.W.P.

References and Notes

(1) Carpenter, S.; Kraus, G. A. *Photochem. Photobiol*. **1991**, *53*, 169−174.
(2) Meruelo, D.; Lavie, G.; Lavie, D.; *Proc. Natl. Acad. Sci. U.S.A.* **1988**, *85*, 5230−5234.
(3) Lavie, G.; Valentine, F.; Levin, B.; Mazur, Y.; Gallo, G.; Lavie, D.; Weiner, D.; Meruelo, D. *Proc. Natl. Acad. Sci. U.S.A.* **1989,** *86*, 5963−5967.
(4) Hudson, J. B.; Lopez-Bazzocchi, I.; Towers, G. H. N.; *Antiviral Res.* **1991,** *15*, 101−112. (b) Hudson, J. B.; Zhou, J.; Chen, J.; Harris, L.; Yip, L.; Towers, G. H. N. *Photochem. Photobiol*. **1994,** *60*, 253−255.
(5) Lopez-Bazzocchi, I.; Hudson, J. B.; Towers, G. H. N. *Photochem. Photobiol*. **1991,** *54*, 95−98.
(6) Degar, S.; Prince, A. M.; Pascaul, D.; Lavie, G.; Levin, B.; Mazur, Y.; Lavie, D.; Ehrlich, L. S.; Carter, C.; Meruelo, D. *AIDS Res. Hum. Retroviruses* **1992,** *8*, 1929−1936.
(7) Meruelo, D.; Degar, S.; Amari, N.; Mazur, Y.; Lavie, D.; Levin, B.; Lavie, G. In Natural Products as Antiviral Agents; Chu, C. K., Cutler, H. G., Eds.; Plenum Press: New York, 1992; pp 91−119.
(8) Treating AIDS with Worts. *Science* **1991**, *254*, 522.
(9) Thomas, C.; Pardini, R. S. *Photochem. Photobiol*. **1993**, *55*, 831−837.
(10) Thomas, C.; MacGill, R. S. Miller, G. C.; Pardini, R. S. *Photochem. Photobiol*. **1992**, *55*, 47−53.
(11) Lenard, J.; Rabson, A.; Vanderoef, R. *Proc. Natl. Acad. Sci. U.S.A.* **1993**, *90*, 158−162.
(12) Kreitmair, H. *Pharmazie* **1950**, *5*, 556−557.
(13) Linde, K.; Ramirez, G.; Mulrow, C. D.; Pauls, A.; Weidenhammer, W.; Melchart, D. *Br. Med. J*. **1996**, *313*, 253−257.
(14) Suzuki, O.; Katsumata, Y.; Oya, M.; Bladt, S.; Wagner, H. *Planta Medica* **1984**, *50*, 272−274.
(15) Anker, L.; Gopalakrishna, R.; Jones, K. D.; Law, R. E.; Couldwell, W. T. *Drugs Future* **1995**, *20*, 511−517.
(16) Gai, F.; Fehr, M. J.; Petrich, J. W. *J. Am. Chem. Soc.* **1993**, *115*, 3384−3385.
(17) Gai, F.; Fehr, M. J.; Petrich, J. W. *J. Phys. Chem*. **1994**, *98*, 5784−5795.
(18) Gai, F.; Fehr, M. J.; Petrich, J. W. *J. Phys. Chem*. **1994**, *98*, 8352−8358.
(19) English, D. S.; Zhang, W.; Kraus, G. A.; Petrich, J. W. *J. Am. Chem. Soc*. **1997**, *119*, 2980−2986.
(20) English, D. S.; Das, K.; Zenner, J. M.; Zhang, W.; Kraus, G. A.; Larock, R. C.; Petrich, J. W. *J. Phys. Chem. A* **1997**, *101*, 3235−3240.
(21) Das, K.; English, D. S.; Fehr, M. J.; Smirnov, A. V.; Petrich, J. W. *J. Phys. Chem*. **1996**, *100*, 18275−18281.
(22) Das, K.; English, D. S.; Petrich, J. W. *J. Am. Chem. Soc*. **1997**, *119*, 2763−2764.
(23) Das, K.; English, D. S.; Petrich, J. W. *J. Phys. Chem. A* **1997**, *101*, 3241−3245.
(24) English, D. S.; Das, K.; Ashby, K. D.; Park, J.; Petrich, J. W.; Castner, E. W., Jr. *J. Am. Chem. Soc*. **1997**, *119*, 11585−11590.
(25) Das, K.; Dertz, E.; Paterson, J.; Zhang, W.; Kraus, G. A.; Petrich, J. W. *J. Phys. Chem. B* **1998**, *102*, 1479−1484.
(26) Carpenter, S.; Fehr, M. J.; Kraus, G. A.; Petrich, J. W. *Proc. Natl. Acad. Sci. U.S.A.* **1994**, *91*, 12273−12277.
(27) Kraus, G. A.; Zhang, W.; Fehr, M. J.; Petrich, J. W.; Wannemuehler, Y.; Carpenter, S. *Chem. Rev*. **1996**, *96*, 523−535.
(28) Duran, N.; Song, P.-S. *Photochem. Photobiol*. **1986**, *43*, 677−680.
(29) Diwu, Z. *Photochem. Photobiol*. **1995**, *61*, 529−539.
(30) Lown, J. W. *Can. J. Chem*. **1997**, *75*, 99−119.
(31) Foote, C. S. In *Light-Activated Pesticides*; Heitz, J. R., Downum, K. R., Eds.; American Chemical Society: Washington, DC, 1987; p 22.
(32) Racinet, H.; Jardon, P.; Gautron, R. *J. Chim. Phys*. **1988**, *85*, 971−977.
(33) Hadjur, C.; Richard, M. J.; Parat, M. O.; Favier, A.; Jardon, P. *J. Photochem. Photobiol. B Chem*. **1995**, *27*, 139−146.
(34) Malkin, J.; Mazur, Y. *Photochem. Photobiol*. **1993**, *57*, 929−933.

(35) Weiner, L.; Mazur, Y. *J. Chem. Soc., Perkin Trans.* **1992**, *2*, 1439−1442.
(36) Diwu, Z.; Lowen, J. W. *Free Rad. Biol. Med*. **1993**, *14*, 209−215.
(37) Weiner, L.; Mazur, Y. *J. Chem. Soc., Perkin Trans. 2* **1992**, *9*, 1439−1442.
(38) Fehr, M. J.; Carpenter, S. L.; Petrich, J. W. *Biorg. Med. Chem. Lett.* **1994**, *4*, 1339−1344.
(39) Fehr, M. J.; McCloskey, M. C.; Petrich, J. W. *J. Am. Chem. Soc*. **1995**, *117*, 1833−1836.
(40) Fehr, M. J.; Carpenter, S. L.; Wannemuehler, Y.; Petrich, J. W. *Biochemistry*, **1995**, *34*, 15845−15848.
(41) Sureau, F.; Miskovsky, P.; Chinsky, L.; Turpin, P. Y. *J. Am. Chem. Soc*. **1996**, *118*, 9484−9487.
(42) Chaloupka, R.; Sureau, F.; Kocisova, E.; Petrich, J. W. *Photochem. Photobiol*., in press.
(43) Hudson, J. B.; Imperial, V.; Haugland, R. P.; Diwu, Z. *Photochem. Photobiol*. **1997**, *65*, 352−354.
(44) Darmanyan, A. P.; Burel, L.; Eloy, D.; Jardon, P. *J. Chim. Phys*. **1994**, *91*, 1774−1785.
(45) Pinto, L. H.; Holsinger, L. J.; Lamb, R. A. *Cell* **1992**, *69*, 517−528.
(46) Newell, K. J.; Tannock, I. F. *Cancer Res*. **1989**, *49*, 4447−4482.
(47) Newell, K. J.; Wood, P.; Stratford, I.; Tannock, I. *Br. J. Cancer* **1992**, *66*, 311−317.
(48) Barry, M. A.; Reynold, J. E.; Eastman, A. *Cancer Res.* **1993**, *53*, 2349−2357.
(49) Li, J.; Eastman, A. *J. Biol. Chem*. **1995**, *270*, 3203−3211.
(50) Gottlieb, R. A.; Nordberg, J.; Skowronski, E.; Babior, B. M. *Proc. Natl. Acad. Sci. U.S.A.* **1996**, *93*, 654−658.
(51) Miccoli, L.; Oudard, S.; Sureau, F.; Poirson, F.; Dutrillaux, B.; Poupon, M. F. *Biochem. J.* **1996**, *313*, 957−962.
(52) Mikovsky, P.; Sureau, F.; Chinsky, L.; Turpin, P.-Y. *Photochem. Photobiol*. **1995**, *62*, 546−549.
(53) Sanchez-Cortes, S.; Miskovsky, P.; Jancura, D.; Bertoluzza, A. *J. Phys. Chem.* **1996**, *100*, 1938−1944.
(54) Sureau, F.; Moreau, F.; Millot, J.-M.; Manfait, M.; Allard, B.; Aubard, J.; Schwaller, M.-A. *Biophys. J*. **1993**, *65*, 1767−1774.
(55) Miskovsky, P.; Chinsky, L.; Wheeler, G. V.; Turpin, P.-Y. *J. Biomol. Struct. Dynam.* **1995**, *13*, 547−552.
(56) Senthil, V.; Longworth, J. W.; Ghiron, C. A.; Grossweiner, L. I. *Biochim. Biophys. Acta* **1992**, *1115*, 192−200.
(57) Falk, H.; Meyer, J. *Monatsh. Chem*. **1994**, *125*, 753−762.
(58) Miskovsky, P.; Sanchez-Cortes, S.; Jancura, D.; Kocisova, E.; Chinsky, L. *J. Am. Chem. Soc*., in press.
(59) Knox, R. S.; Gulen, D. *Photochem. Photobiol*. **1993**, *57*, 40−43.
(60) Wynne, K.; Hochstrasser, R. M. *Chem. Phys*. **1993**, *171*, 179−188.
(61) Song, Q.; Harms, G. S.; Wan, C.; Johnson, C. K. *Biochemistry*, **1994**, *33*, 14026−14033.
(62) Savikhin, S.; Tao, N.; Song, P.-S.; Struve, W. S. *J. Phys. Chem*. **1993**, *97*, 12379−12386.
(63) Freeman, D.; Frolow, F.; Kapinus, E.; Lavie, D.; Lavie, G.; Meruelo, D.; Mazur, Y. *J. Chem. Soc., Chem. Commun*. **1994**, 891.
(64) The designation of "back transfer" is based upon the assumption in the literature that the most stable form of hypocrellin is that illustrated in Figure 1g. The published X-ray structure indicates C(12)−O(12) and C(7)−O(7) bond lengths that are within experimental error greater than those of their C(1)−O(1) and C(6)−O(6) neighbors.[65] The coordinates available from the Cambridge Crystallographic Data Bank suggest that all four bond lengths are comparable. The former data set is consistent with Figure 1h, enol bonds being longer than keto bonds. The latter data set suggests a mixture of both the normal and the tautomer forms in the ground state.
(65) Wei-shin, C.; Yuan-teng, C.; Xiang-yi, W.; Friedrichs, E.; Puff, H.; Breitmaier, E. *Liebigs Ann. Chem.* **1981**, 1880−1885.
(66) Borgis, D.; Hynes, J. T. In *The Enzyme Catalysis Process*; Cooper, A., Houben, J. L., Chien, L. C., Eds.; NATO ASI Series; Plenum Press: New York, 1989; Vol. 178, p 293.
(67) Borgis, D.; Hynes, J. T. *J. Chem. Phys*. **1991**, *94*, 3619−3628.
(68) Azzouz, H.; Borgis, D. *J. Chem. Phys.* **1993**, *98*, 7361−7374.
(69) Staib, A.; Borgis, D.; Hynes, J. T. *J. Phys. Chem.* **1995**, *99*, 2487−2505.
(70) Etzlstorfer, C.; Falk, H.; Müller, N.; Schmitzberger, W.; Wagner, U. G. *Monatsh. Chem*. **1993**, *124*, 751−761. (b) Falk, H. Personal communication.
(71) We had previously reported that hypericin does not require oxygen for its antiviral activity.[24,27,38,40] This conclusion was based on the inability to estimate accurately low oxygen levels in our virus samples. We consequently now believe that while antiviral pathways independent of oxygen may exist, the role of oxygen in this activity is significant. The ability of photogenerated protons to enhance the activity of activated oxygen species[42] is still considered to be of importance (Park, J.; English, D. S.; Wannemuehler, Y.; Carpenter, S.; Petrich, J. W. *Photochem. Photobiol.*, in press.)
(72) Chuang, M. C.; Eisenthal, K. B. *J. Chem. Phys.* **1972**, *57*, 5094−5097.
(73) Eloy, D.; Le Pellec, A.; Jardon, P. *J. Chim. Phys*. **1996**, *93*, 442−457.
(74) Altmann, R.; Falk, H. *Monatsh. Chem*. **1997,** *128*, 571−583.
(75) **7**5. Yamazaki, T.; Ohta, N.; Yamazaki, I.; Song, P.-S. *J. Phys. Chem*. **1993**, *97*, 7870−7875.
(76) Zhang, M.-H.; Weng, M.; Chen, S.; Xia, W.-L.; Jiang, L.-J.; Chen, D.-W. *J. Photochem. Photobiol. A: Chem.* **1996**, *96*, 57−63.
(77) Redepenning, J.; Tao, N. *Photochem. Photobiol*. **1993**, *58*, 532−535.
(78) Burel, L.; Jardon, P.; Lepretre, J.-C. *New. J. Chem*. **1997**, *21*, 399−403.
(79) Wells, T. A.; Losi, A.; Dai, R.; Scott, P.; Park, S.-U.; Golbeck, J.; Song, P.-S. *J. Phys. Chem. A* **1997**, *101*, 366−372.
(80) (a) Turro, C.; Chang, C. K.; Leroi, G. E.; Cukier, R. I.; Nocera, D. G. *J. Am. Chem. Soc.* **1992**, *114*, 4013−4015. (b) O'Conner, D.; Shafirovich, V. Ya.; Geacintov, N. E. *J. Phys. Chem*. **1994**, *98*, 9831−9839.
(81) Diwu, Z.; Lown, J. W. *J. Photochem. Photobiol. A: Chem*. **1992**, *64*, 273−287.